2020 IMEKO TC-4 International Conference on
Metrology for Archaeology and Cultural Heritage
Trento, Italy, October 22-24, 2020

Effect of age on Pine wood microstructure studied by micro-MRI and diffusion-NMR

Valeria Stagno[1,2], Sveva Longo[2,3], Silvia Capuani[2]

[1] *Earth Sciences Department, Sapienza University of Rome, Piazzale Aldo Moro 5, 00185 Rome, Italy, valeria.stagno@uniroma1.it*
[2] *National Research Council - Institute for Complex Systems (CNR-ISC) c/o Physics Department Sapienza University of Rome, Piazzale Aldo Moro 5, 00185 Rome, Italy.*
[3] *Department of Mathematical and Computational Sciences, Physics Science and Earth Sciences (MIFT), University of Messina, 98166 Messina, Italy.*

***Abstract* – Wood is a natural complex material widely used from men in the past to create artworks. One of its main anatomical elements is the annual ring that varies according to the species, the weather conditions under which the tree has grown and to possible adversities. To observe the anatomy of waterlogged archaeological wood could be complicated because of its degradation. However, knowing the state of conservation is very important for the future restoration. In this work a non-destructive approach based on the combined use of MRI and diffusion on the modern and ancient pine wood is presented. Micro-MR images allow to observe the diagnostic features. The molecular NMR diffusion analysis, with the estimation of the pores diameter and the tortuosity, provide important information about the effect of age on the wood microstructure. At the end of the analysis the unaltered sample can be repositioned in its original location on the artwork.**

I. INTRODUCTION

Wood is a natural porous material with a complex morphology. In the past, it has been widely used from men to produce artworks. For this reason, wood is widespread in the Cultural Heritage world and its microstructure has always been studied for the species identification, for dendrochronological analyses and for extracting important information about ancient human activities [1]. Two principal types of wood can be recognized: softwood and hardwood. Softwood has a very homogeneous structure mainly composed of tracheids and fibre-tracheids [2]. The resin canals are one of its main characteristics that allow it to be distinguished from the hardwood. In addition, its annual rings are usually well separated through the annual ring limit and they are made of an earlywood area, with pores characterized by larger lumens and thinner walls, and a latewood area with thicker walls and smaller lumens [2]. However, these two areas are not always well differentiated. Some softwoods present an abrupt passage from earlywood to latewood, while some others a gradual one [2]. Among the many anatomical elements described above, the growth ring is for sure one of the most important because its characterization provides the age of the tree and the climatic conditions in which it has grown [3], as well as being crucial for the species identification. Waterlogged degraded wood is usually well preserved for the microscopic observation of its annual rings. Conversely, at a macroscopic level the wood rings are not always visible with the naked eye because of the wood structure changes in colour, consistency and superficial morphology [4]. Moreover, the evaluation of the effect of age is also very important for example to determine the conservation state of an artwork. To know the state of a wooden remain can be useful for planning the restoration and choosing the restoration materials [5]. The aim of this work was to evaluate the decay of pine wood through the comparison of MR images and diffusion analyses of a modern and an archaeological sample. The MR images allow an alternative and non-destructive approach for the characterization of the annual rings, as well as of all the diagnostic features, of waterlogged wood. The diffusion analysis [6-9], with the estimation of the pores diameter and the tortuosity, provide important information about the effect of age and the decay process of the wood microstructure. At the end of the analysis the unaltered sample can be repositioned in its original location on the artwork.

II. MATERIALS AND METHODS

Two cylinders-like wood samples of a soaked modern wood and an archaeological waterlogged wood were studied. Their size was less than 15 mm in length and 8 mm in diameter, well suitable for a 10 mm NMR tube. The

archaeological sample detached from an ancient pole of the Roman harbour of Naples, dated to the V century AD [10, 11]. It was well preserved in waterlogged conditions and for this reason was always kept in water during the analysis. The modern wood, instead, was previously maintained at the environmental conditions of 20°C and 50% of relative humidity. In order to perform the MRI and diffusion acquisitions, the modern sample was imbibed with distilled water until the saturation was reached. Both the species of modern and archaeological wood was stone pine (*Pinus Pinea*) [12, 13]. For the acquisition of MR images, the samples were inserted with distilled water in the NMR tube and sealed with parafilm in order to prevent water evaporation. All the experiments were performed with a 400 MHz Bruker-Avance spectrometer with a 9.4 T magnetic field and a micro-imaging unit equipped with high-performance and high-strength magnetic field gradients for MRI and diffusion measurements. The gradients maximum strength was 1200 mT/m and the rise time 100 µs. T_2*-weighted images were performed with a Gradient Echo Fast Imaging (GEFI) sequence [6] in the transversal and radial direction. The optimized parameters used in the GEFI sequence are reported in Table 1, where TE is the echo time, TR the repetition time, NEX the number of scans, STK the slice thickness, FOV the field of view, MTX the image matrix, R the in plane resolution.

Table 1. Acquisition parameters of GEFI sequences.

	Modern Pine	Archaeo Pine
TE/TR (ms)	3/1200	5/1500
Number of Slice	3	3
NEX	128	128
STK (µm)	200	300
FOV (cm^2)	0.9x0.9 / 1.4x1.4	0.9x0.9
MTX (pixels)	512x512	512x512
R (μm^2)	18x18 / 27x27	18x18

For the measurement of the water diffusion coefficient, a Pulse Gradient Stimulated Echo (PGSTE) sequence [8, 9] was used. The diffusion was measured along the x axis (i.e. perpendicular to the main direction of the wood grain). The PGSTE signal was obtained using TR=5 s, TE= 1.9 ms, diffusion gradient pulse (δ)=3ms, 32 steps of the gradient strength (g), from 26 to 1210 mT/m, for each diffusion time (Δ). The Δ values used were 0.04 - 0.08 - 0.12 - 0.16 - 0.2 - 0.3 - 0.4 - 0.6 - 0.8 - 1.0 s. The b-value, defined as $b = y^2 g^2 \delta^2 (\Delta-\delta/3)$, spanned from a minimum of 1.6 x 10^7 s/m^2 to a maximum of 9.5 x 10^{11} s/m^2.

A. Data Processing

The diffusion data was elaborated with OriginPro 8.5 software where the diffusion coefficient values were obtained by fitting the NMR signal S(g) as function of the b-value by the following equation:

$$S(g)=M_1 \exp(-D_1 b)+M_2 \exp(-D_2 b) \quad (1)$$

Where S(g) is the NMR signal as function of the gradient strength, D_1 and D_2 are the two components of the diffusion coefficient associated with the magnetizations M_1 and M_2, respectively. The fit goodness was evaluated by the $\bar{R}^2$ (i.e. the R^2 corrected for the number of the regressors).

Plots of the diffusion coefficient (D) vs. the diffusion time (Δ) and the magnetizations (M) vs. the diffusion time (Δ) were performed with MatlabR2019b.

From the D vs. Δ trend, the first and last points, corresponding to the free water diffusion and the diffusion through semi-permeable membranes (i.e. the wood cell walls), were removed and the pores radius (L) was estimated by the linear fit of D(Δ) vs. $2\Delta^{-1}$:

$$D(\Delta) = \frac{L^2}{2\Delta} \quad (2)$$

From the pores radius (L) of Eq.(2), the pores diameter (d) was calculated.

In addition, the value for Δ=∞ of the normalized diffusion coefficient D/D_0, where D_0 is the free water diffusion coefficient equal to $2.3x10^{-9}$ m^2/s, was calculated and used to evaluate tortuosity according to the equation:

$$\tau = \frac{D_0}{D_\infty} \quad (3)$$

Tortuosity is an intrinsic property of a porous material usually defined as the ratio of actual flow path length to the straight distance between the ends of the flow path. So, τ of the porous system reflects the connectivity degree of the porous network [14-16].

III. RESULTS

T_2*-weighted images of the transversal and radial section of modern stone pine are displayed in Fig. 1a) and 1b), respectively. Here, several anatomical elements are observable. First of all, in Fig. 1a) the annual rings limit (white arrow) is well visible with two areas with a different contrast. The darker area corresponds to structures with low T_2* values, while the brighter ones to structures with high T_2* values [17]. The dark area is the latewood (light blue circle) while the bright area is the earlywood (green circle). The other larger pores are the resin canals (red circle) and also the rays (pink arrow) can be observed. In the radial section of Fig. 1b) only the annual rings limits (white arrow) can be seen.

T_2*-weighted images of the transversal and radial section of archaeological stone pine are displayed in Fig. 2a) and 2b), respectively. In Fig. 2a) the presence of many black spots (yellow circles) identified as fungal attacks and paramagnetic impurities, due to the long period of burial under the sediments of the seabed, is clearly visible [18]. It is possible to observe all the anatomical elements of the transversal section, such as the darker areas of latewood

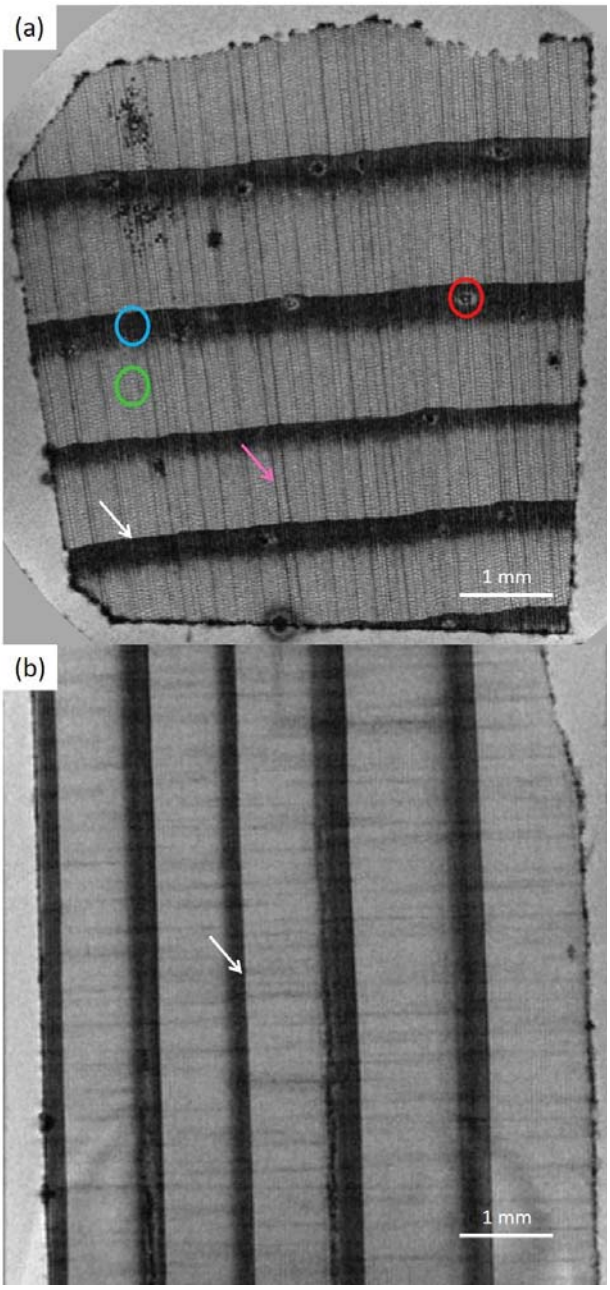

Fig. 1. T_2-weighted images of the modern pine. In (a) the transversal section shows the resin canals (red circle), the earlywood (green circle), the latewood (light blue circle), the rays (pink arrow) and the annual ring limit (white arrow). In (b) the radial section presents the annual ring limit (white arrow).*

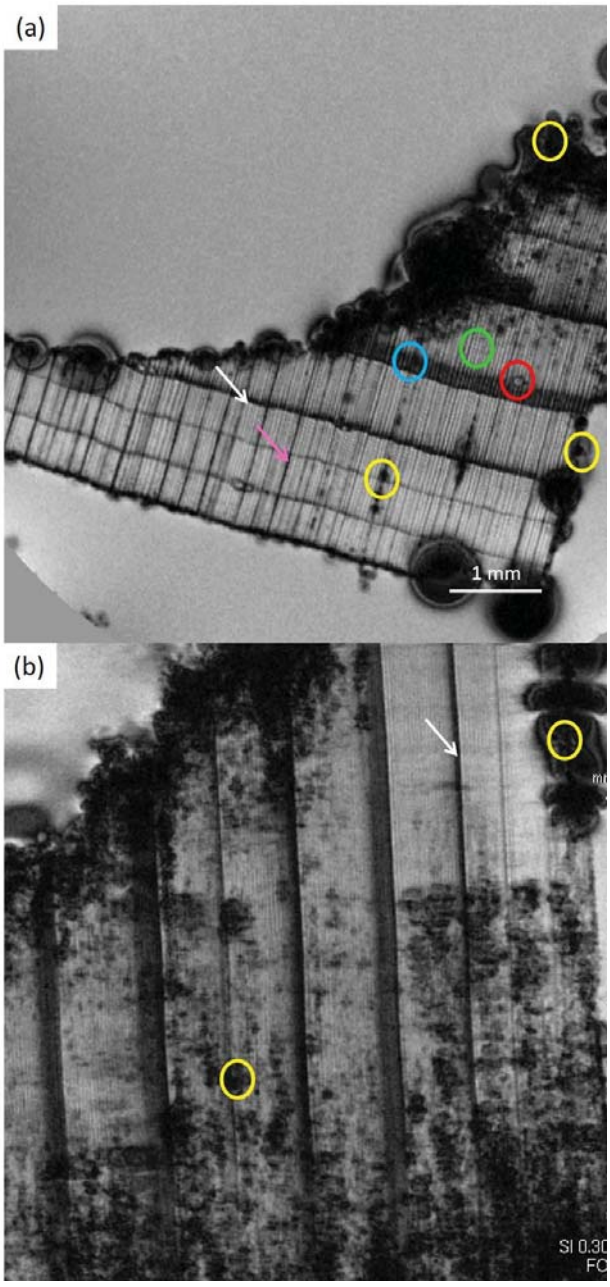

Fig. 2. T_2-weighted images of the archaeological pine. In (a) the transversal section shows the resin canals (red circle), the earlywood (green circle), the latewood (light blue circle), the rays (pink arrow) and the annual ring limit (white arrow). There are also impurities and fungi highlighted by yellow arrows. In (b) the radial section presents the annual ring limit (white arrow) and impurities and fungi (yellow circles).*

(light blue circle), the brighter areas of earlywood (green circle), the resin canals and rays (red circle and pink arrow). In the radial section of Fig. 2b) the growth rings limits (white arrow) are displayed.

In Fig. 3a) and 3b) the first (Dx_1) and second (Dx_2) diffusion component as function of the diffusion time DELTA are displayed. In Fig. 4a) and 4b) the magnetizations M_1 and M_2 as function of DELTA and associated with D_1 and D_2, are shown.

In Table 2 the pores diameter and the tortuosity calculated by Eq.(2) and Eq.(3), respectively, are reported. In Table 2 the magnetizations associated with each pores size are also shown.

IV. DISCUSSIONS

From the comparison of the transversal and radial section of the modern (Fig.1a and 1b) and the ancient (Fig.2a and

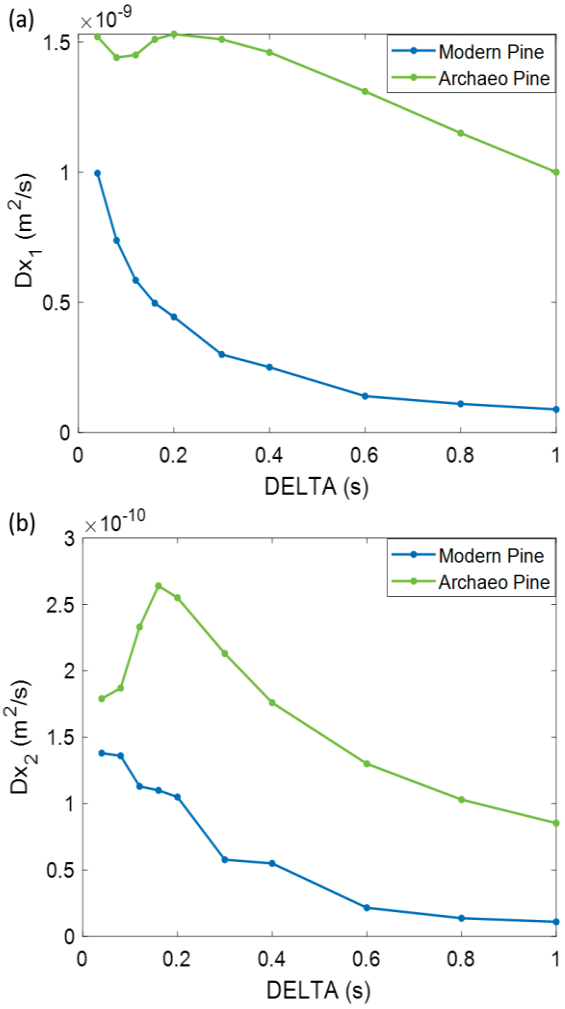

Fig. 3 The first (a) and the second (b) component of the water diffusion coefficient along x as function of the diffusion time DELTA.

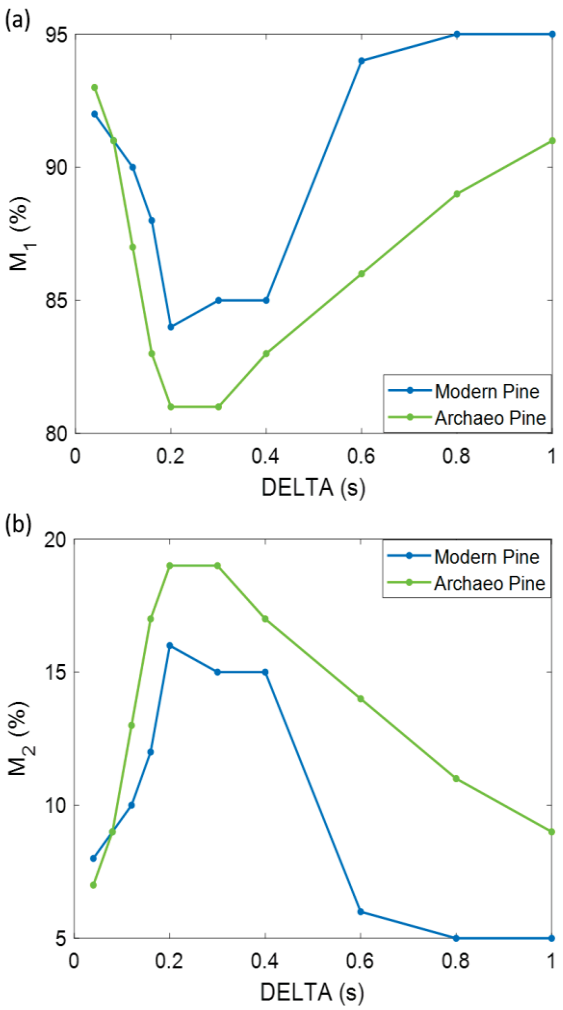

Fig. 4 The first (a) and the second (b) magnetization associated with the water diffusion coefficient along x as function of the diffusion time DELTA.

2b) pine it is possible to notice some differences. First of all, the already mentioned black spots (see section III), can be associated with a degradation process operated by fungi and with the accumulation of paramagnetic impurities (metals and salts) from the burial place inside the wood structure.

These black zones are not present in the modern wood and they are mostly located along the rays and on the edge of the sample (Fig. 2a, 2b yellow circles). This indicates a strong fungal attack and deposition of impurities in these zones. The image contrast allows to observe that both the woods show well delimited growth rings. While the modern wood does not show particular changes in the annual ring thickness, in Fig. 2a the ancient pine has some thinner annual rings with no latewood. This may be due to a climatic change during the tree growth (before the V century AD). In fact, thinner rings are usually attributed to not rainy periods [4].

The plots of the diffusion coefficient vs. the diffusion time in Fig. 3a and 3b show that both the woods have two main diffusion compartments but the diffusion in the modern pine is slower than that in the ancient pine. The difference is around one order of magnitude for both the compartments (Dx_1 and Dx_2). This situation can be explained as the consequence of the degradation process that occurred in the ancient pine. In fact, the decay of the cellular structure and wood polymers may have produced the cell walls thinning and the lumens enlargement in the archaeological pine. Both the woods have two main pores sizes as shown in Table 2 where the two sizes (d1 and d2) can be identified as the earlywood and latewood tracheids diameter. By comparing the diameters of the modern and the ancient pine, it is clear that there is an increment of the pores size both in earlywood and latewood for the archaeological pine. However, the latewood tracheids seem to be more affected by this enlargement. A possible explanation is that the decay is higher in areas with a high concentration of wood polymers, such as the latewood cell walls. This means that the greater the thickness of the cell wall, the greater its deterioration. The magnetizations associated with each diameter are a good tool to quantify the porosity. For both the pines, the earlywood tracheids

Table 2. Pores diameters, magnetizations and tortuosity.

	d_1 (μm)	d_2 (μm)	M_1 (%)	M_2 (%)	τ
Modern Pine	25.2±0.9	12.8±0.8	89±2	11±2	18.4
Archaeo Pine	27.1±4.8	17.9±1.9	84±1	16±1	1.9

(~85%) are more abundant than the latewood tracheids (~15%), in agreement with the MR images (Fig. 1a and 2a).

Further information can be deduced from the tortuosity (τ) (Table 2). The modern pine shows a higher tortuosity compared to the archaeological pine. This is in good agreement with the diffusion coefficient and diameters results. In fact, the higher the tortuosity, the more complicated the water routes. This means that the modern wood has a complex structure within which water cannot move easily. Conversely, the ancient pine has lost this complexity because of the structures degradation that has produced new voids and widened the existing pores lumens making the water motion easier.

V. CONCLUSIONS

In this work we suggest that the combined use of NMR-diffusion and micro-MRI can help in the non-invasive characterization of waterlogged archaeological wood. By comparing the modern pine sample and the ancient pine sample, the effect of the degradation process on the wood microstructure can be observed through the MR images and quantified by the diffusion coefficient of water and tortuosity. This new approach revealed that the decay mostly occurs in areas with a high concentration of polymers, such as rays and latewood cell walls, with the enlargement of the pores lumen and the loss of wood complexity. MRI can also reveal morphological aspects of wood, such as the annual rings, that can inform about past climate changes.

ACKNOWLEDGMENTS

The authors would like to thank the Istituto Centrale per il Restauro (ICR) of Rome (Italy) for providing the archaeological wood sample.

REFERENCES

[1] English Heritage, “Waterlogged wood guidelines on the recording, sampling, conservation and curation of waterlogged wood”, English Heritage Publishing, 2010.

[2] H.G. Richter, D. Grosser, I. Heinz, P.E. Gasson, “Iawa list of microscopic features for softwood identification ” IAWA J., 2004, vol.25, pp. 1–70.

[3] http://www.climatedata.info/proxies/tree-rings/, 2020 (accessed 25 June 2020).

[4] D.M. Pearsall, “Paleoethnobotany, Third Edition: A Handbook of Procedures”, 3rd edition, Routledge, 2015.

[5] T. Nilsson, R. Rowell, “Historical wood – structure and properties”, Journal of Cultural Heritage, 2012, vol.13, pp. S5–S9.

[6] P.T. Callaghan, “Principles of Nuclear Magnetic Resonance Microscopy”, Oxford University Press Inc, New York, 1991.

[7] W.S. Price, “NMR studies of translational motion: principles and applications”, Cambridge University Press, Cambridge, 2009.

[8] E. O. Stejskal, J. E. Tanner, “Spin Diffusion Measurements: Spin Echoes in the Presence of a Time Dependent Field Gradient”, J. Chem. Phys., 1965, vol.42, pp. 288-292.

[9] P. N. Sen, “Time-Dependent Diffusion Coefficient as a Probe of Geometry”, Concepts in Magnetic Resonance, 2004, vol.23A, pp. 1-21.

[10] V. Di Donato, M.R. Ruello, V. Liuzza, V. Carsana, D. Giampaola, M.A. Di Vito, C. Morhange, A. Cinque, E. Russo Ermolli, “Development and decline of the ancient harbor of Neapolis”, Geoarchaeology, 2018, vol.33, pp. 542–557.

[11] D. Giampaola, V. Carsana, G. Boetto, F. Crema, C. Florio, D. Panza, M. Bartolini, C. Capretti, G. Galotta, G. Giachi, et al., “La scoperta del porto di" Neapolis": dalla ricostruzione topografica allo scavo e al recupero dei relitti”, Archaeol. Maritima Mediterr., 2005, vol.2, pp. 1000–1045.

[12] InsideWood.2004-onwards. http://insidewood. lib.ncsu.edu/search, 2020 (accessed 20 July 2020).

[13] Wood anatomy of central European species. http://www.woodanatomy.ch , 2020 (accessed 20 July 2020).

[14] F. A. L. Dullien, “Porous Media: Fluid Transport and Pore Structure”, Academic, New York, 1979.

[15] P. P. Mitra, P. N. Sen, L. M. Schwartz, P. Ledoussal, “Diffusion Propagator as a Probe of the Structure of Porous Media”, Phys. Rev. Lett., 1992, vol.68, pp. 3555–3558.

[16] M. Zecca, S. J. Vogt, P. R. Connolly, E. F. May, M. L. Johns, “NMR Measurements of Tortuosity in Partially Saturated Porous Media”, Transport in Porous Media, 2018, vol.125, pp. 271-288.

[17] P.M. Kekkonen, V.-V. Telkki, J. Jokisaari, “Determining the Highly Anisotropic Cell Structures of Pinus Sylvestris in Three Orthogonal Directions by PGSTE NMR of Absorbed Water and Methane”, J. Phys. Chem. B, 2009, vol.113, No.4, pp. 1080.

[18] S. Capuani, V. Stagno, M. Missori, L. Sadori, S. Longo, “High-resolution multiparametric MRI of contemporary and waterlogged archaeological wood”, Magn Reson Chem., 2020, vol.58, pp. 860-869.